Journal Pre-proofs

Excited State Hydrogen Atom Transfer Pathways in 2,7-Diazaindole – S_{1-3} ($S=H_2O$ and NH_3) Clusters

Simran Baweja, Prahlad Roy Chowdhury, Surajit Maity

PII: S1386-1425(21)00963-X
DOI: https://doi.org/10.1016/j.saa.2021.120386
Reference: SAA 120386

To appear in: *Spectrochimica Acta Part A: Molecular and Biomolecular Spectroscopy*

Received Date: 26 April 2021
Revised Date: 17 August 2021
Accepted Date: 6 September 2021

Please cite this article as: S. Baweja, P. Roy Chowdhury, S. Maity, Excited State Hydrogen Atom Transfer Pathways in 2,7-Diazaindole – S_{1-3} ($S=H_2O$ and NH_3) Clusters, *Spectrochimica Acta Part A: Molecular and Biomolecular Spectroscopy* (2021), doi: https://doi.org/10.1016/j.saa.2021.120386

Excited State Hydrogen Atom Transfer Pathways in 2,7-Diazaindole – S_{1-3} ($S=H_2O$ and NH_3) Clusters

Simran Baweja,[1] Prahlad Roy Chowdhury,[2] Surajit Maity*

Department of Chemistry, IIT Hyderabad, Kandi, Sangareddy, Telangana, India, PIN-502285

*Email: surajitmaity@chy.iith.ac.in

Abstract:

The photoinduced tautomerization reactions via hydrogen atom transfer in the excited electronic state (ESHT) have been computationally investigated in 2,7-diazaindole; 27DAI – $(H_2O)_{1-3}$ and 27DAI – $(NH_3)_{1-3}$ isolated clusters to understand the role of various solvent wires. Two competing ESHT reaction pathways originating from the N(1)-H group to the neighbouring N(7) ($R_{(1H\text{-}Sn\text{-}7H)}$) and N(2) ($R_{(1H\text{-}Sn\text{-}2H)}$) atoms were rigorously examined for each system. Both one- and two-dimensional potential energy surfaces have been calculated in the excited state to investigate the pathways. The $R_{(1H\text{-}Sn\text{-}7H)}$ was found to be the dominant route with reaction barriers ranging from 26-40 kJmol^{-1} for water clusters, while the reaction barrier for ammonia was at 14-26 kJmol^{-1}, nearly half of the barrier heights calculated for the water system. The lengthening of the solvent chain up to two molecules resulted in a drastic decrease in the barrier heights for $R_{(1H\text{-}Sn\text{-}7H)}$. The barriers of the competing reaction channel $R_{(1H\text{-}Sn\text{-}2H)}$

[1,2] These authors contributed equally

were found to be significantly higher (31-127 $kJmol^{-1}$) but were observed to be decreasing with the lengthening of the solvent wire as in the $R_{(1H\text{-}Sn\text{-}7H)}$ pathway. In both the reactions, the angle strain present in the transition state structures was dependent upon the solvent chain's length and was most likely the governing factor for the barrier heights in each solvent cluster. The results have also affirmed that the ammonia molecule is a better candidate for hydrogen transfer than water because of its higher gas-phase basicity. The results delineated from this investigation can pave the way to unravel the excited-state hydrogen transfer pathways in novel N-H bearing molecules.

Keywords: Excited-state hydrogen atom transfer reaction, 2D-potential energy surface, Reaction Pathway, non-covalent interaction, Hydrogen bonding, Isolated micro-solvated molecular clusters

1. Introduction

Excited-state proton and hydrogen atom transfer reactions have swiftly gained recognition due to their immense applications in various practical fields such as fluorescent chemosensors,[1–3] photo-stabilizers,[4] light-emitting diodes,[5] laser dyes,[6] molecular switches,[7,8] organic optoelectronic materials,[9] among many others. The photoinduced tautomerization is the key phenomenon that biomolecules undergo upon UV irradiation.[10,11] Solvent-assisted proton and hydrogen atom transfer (ESHT) reactions involving site-specific hydrogen bonding networks have been widely investigated in the solution phase. But to stipulate the role of solvents, ESHT reactions have been investigated experimentally and computationally in the isolated gas-phase clusters over the past couple of decades.[12-15] Substituted indole molecules have been the subject of interest because of their antioxidant, anticancer, antibacterial, antifungal characteristics. The central chromophore of the eumelanin pigments

found in nature is an indole derivative. Nonradiative deactivation of the indole derivatives plays a crucial role to protect organisms from the damaging effect of UV radiation.[16] Photoinduced tautomerization of 7-azaindole derivatives has been extensively investigated over the last two decades because its complexes show hydrogen bonding interaction analogous to the DNA base pairs. The excited state tautomerization via hydrogen and proton transfer reaction may provide the possible mechanisms of the mutation processes in organisms on the exposure to UV radiation.[17]

Recently, several research groups theoretically investigated the possible ESHT reaction pathways present in water clusters of 2,6-DAI, 2,7-DAI and 7-AI.[12-14,18] Fang et al. reported that in isolated 7-AI complexes with protic solvents, ammonia is a better proton acceptor when compared to other solvents due to its high gas-phase basicity.[19] The substitution of the pyrrole moiety of 7-AI with a pyrazole in 2,7-DAI extensively decreases the barrier in the excited state as the electron-withdrawing N-atom at the '2'-position increases the acidity of N-H proton.[15] The authors reported two competing excited tautomerization processes in the excited state, (a) N(1)-H to N(7) and (b) N(1)-H to N(2). A theoretical investigation by Liu et al. suggested that the ESHT process in 2,7-diazaindole (2,7-DAI) requires a minimum of two water molecules for the N(1)-H to N(7) hydrogen atom transfer.[12] As observed by Shen et al., the N(7)-H tautomer of 2,7-DAI has been characterized by a brighter fluorescence in the aqueous phase compared to that of the 7-AI molecule.[15] From the previous studies, the ESHT energy barriers for 7-AI-$(H_2O)_{1,2}$ were reported to be 73.7 kJmol^{-1} and 63.9 kJmol^{-1} for one and two-water complexes at the B3LYP/6-311G++ level of theory, respectively.[20] But for the 2,7-DAI-$(H_2O)_2$ cluster, the barrier was reported to be 29.2 kJmol^{-1} at the B3LYP/TZVP level of theory which is significantly lower than the 7-AI complexes.[12] The N(1)-H to N(2) pathway was reported to have a higher energy barrier but has not been extensively investigated so far.[21,22]

In the current work, we have vastly curated the solvent-assisted N-H hydrogen atom transfer in 27DAI-S_n (n=1-3) clusters where the solvent molecules (S) are water and ammonia. We have systematically investigated the governing factors of two competing ESHT reaction processes involving a hydrogen atom transfer from the N(1)-H to N(7) and N(2) sites. In addition, we have examined the correlation between the energy barriers and (a) the length of the solvent wire, (b) the type of solvent molecules. A thorough investigation of the competing hydrogen atom transfer energy barriers with the physical properties of solvents is sparse in the literature. This study is essential to investigate the competing ESHT reaction processes with multiple acceptor sites connected via solvent wires.

2. Computational Methods

The geometry optimization in the ground state (S_0) and the first singlet excited state (S_1) for various structures was performed using D4-dispersion corrected DFT and TDDFT methods with Becke's three-parameter hybrid exchange function, the Lee-Yang-Parr gradient-corrected correlation functional (B3-LYP) [23-25] and def2-TZVPP/def2-TZVP basis set.[26,27] The counterpoise corrections for the basis set superposition error were not performed separately as it is incorporated in the D4-correction methods. The optimized geometries in the ground (S_0) and optically bright $\pi\pi^*$ states (S_1 states of 1H-S_n and 7H-S_n, and S_2 state in 2H-S_n complexes) were confirmed as the local minima from all the positive frequencies in the subsequent frequency calculations. The ground transition states were searched along the reaction coordinate and were confirmed from the frequency calculation. In the excited state, the potential energy surfaces (PES) were obtained by local optimization of the $\pi\pi^*$ states while varying both N(1)-H and N(7)-H bond lengths of the 1H-$S_{1\text{-}2}$ and 7H-$S_{1\text{-}2}$ structures sequentially. The above resulted in a 2D-PES, which was further used to identify the lowest energy reaction path. The highest energy structures present in that lowest energy path have

been considered as the excited state TS of the reaction without further investigation. Herein, we have searched for excited state tautomerization reactions (i) 1H-S_n to 7H–S_n (hereafter R(1H-S_n-7H) and (ii) 1H-S_n to 2H–S_n (hereafter R(1H-S_n-2H)) pathways. In addition, we have also explored the 1D-PES for both R(1H-S_n-7H) and R(1H-S_n-2H) pathways using constrained geometry optimization in the ππ* state connecting the reactants and products. All the calculations have been done using the TURBOMOLE software package.[28]

3 Results and Discussion

3.1 27DAI-S_n complexes in the ground state

Figure 1 shows the geometry optimized structures of three 2,7-diazaindole tautomers, 1H-DAI, 2H-DAI, and 7H-DAI. As shown in Table 1, the 1H isomer is the most stable structure in the ground electronic state, which is about 32.6 kJmol^{-1} and 76.5 kJmol^{-1} more stable than the 2H and 7H isomers, respectively. The hydrogen-bonded network of 27DAI-S_{1-3} clusters was obtained by positioning the solvent cluster around the potential binding sites of the 27DAI tautomers. The calculated zero-point vibrational energy (ZVPE) corrected binding energies $D_0(S_0)$ are shown in Table 1. The geometry optimized structures in the ground states are in SI Figure S1-S3. This study focuses upon the energetics of the solvent assisted tautomerization via hydrogen transfer reaction in the excited state. Therefore, detailed analysis of the ground state structures and their respective energies is provided in the supporting information document.

3.2 27DAI-S_n complexes in the electronic ππ* excited state:

The electronic excited S_1 states of 1H and 7H molecules are the optically bright ππ* states. The calculated oscillator strengths of the $S_0 \rightarrow S_1$ vertical transitions in 1H at 269 nm and 7H at 397 nm are 0.045 and 0.015, respectively (SI Table S3). The experimental investigation has shown that the $S_0 \rightarrow S_1$ excitation at 290 nm followed by the 1H-to-7H tautomerization

process resulted in red-shifted fluorescence emission from the tautomeric structure at ~500 nm.[15] The excited states of the tautomers are expected to be predominantly in the ππ* states for the observed radiative emission. The experimentally observed red shift and the relative intensity of the tautomer emission are well correlated with our current data. In the case of the 2H isomer, the first (S_1) and second (S_2) electronically excited states are nπ* and ππ* states, respectively. The associated vertical excitation energies are 299 nm and 289 nm, with oscillator strengths of 0.000 and 0.062, respectively. Experimentally, the 1H-to-2H excited state tautomerization process was confirmed with bright fluorescence emission at 380 nm.[15] The above suggests that the 2H tautomer emission occurs from the excited ππ* state. The observed red-shifted fluorescence emission with respect to the 1H isomer is in good agreement with the current calculated data (SI Table S3). The oscillator strength of the $S_0 \rightarrow S_2$ transition in the 2H isomer is higher than both 1H and 7H tautomers.

Based on the above correlation with experimental data, the structures and energies of the excited states were probed on the ππ* electronic states in all the systems. As shown in Table 1, for the S_1 electronic state (ππ* state), the 7H isomer is more stable by 92.4 $kJmol^{-1}$ compared to the ππ* state (S_1) of 1H isomer. The calculated energies are comparable with the experimental and calculated values for the 2,7DAI, and 7AI isomers, as reported earlier.[12] The relative energy of the ππ* state (S_2) of the 2H isomer is marginally higher than that of the 1H isomer. The calculated vertical excited energies and oscillator strengths of the complexes are shown in SI Table S3.

The optimized geometries in the excited state show different structural parameters for the 1H, 2H and 7H isomers near the hydrogen bond docking sites. As shown in Table 1, the $R_{N(1)\text{-}Ha}$ bond length increases by 0.008 Å. However, the $R_{N(7)\text{-}Hb}$ and $R_{N(2)\text{-}Hb}$ in 7H isomer and 2H isomers are reduced by 0.006 and 0.005 Å, respectively. Figure 1 shows the frontier molecular orbitals of HOMO (π) and LUMO (π*) of all the tautomers. The N(1)-sites depicted

in the HOMO of the tautomers show a higher π-electron density compared to the N(7) and N(2) positions. However, the LUMO shows a decreased electron density at the N(1) position and an increase in electron density at the N(7) and N(2) positions. The above resulted in an increase of N(1)-H bond length upon electronic excitation. In addition, both N(7) and N(2) positions in the S_1 state of 7H and 2H isomers show diminished N(7/2)-H_b bond lengths because of the increased π-electron density on these positions.

In the case of 1H-S_n, 7H-S_n complexes, the S_1 electronic state is a ππ* state. In the case, 2H-S_n complexes (except 2H-A_3), the S_1 and S_2 states are found to be optically dark nπ* and bright ππ* states (SI Table S3), respectively. The excited-state structures are shown in Figures 2-4, and the energy and structural parameters are given in Table 1. In both ground and excited state, the most stable structure in the 1H-S_{1-3} system shows the formation of a solvent wire as N(1)–H_a···S_n···N(7). The structure is named as I_1 isomer in each system. The corresponding tautomer 7H-S_n with an N(7)–H_b···S_n···N(1) linkage is found to be the most stable structure. The second most stable isomer of the 1H-S_n system shows an N(1)–H_a···S_n···N(2) linkage, represented as I_2 isomer. The tautomeric form of IH-S_n(I_2) isomer is 2H-S_n with an N(2)–H_b···S_n···N(1) linkage, which is the most stable structure of the 2H-S_n system.

M-S complexes: Figure 2 depicts the single solvent clusters of 1H, 7H and 2H isomers in the S_1 state. The binding energies and relative energies in the excited states are shown in Table 1. In the ππ* state, the 1H-S(I_1) isomers are 75.6 (S=H_2O) and 74.4 kJmol^{-1} (S=NH_3) less stable than the respective tautomer 7H-S complexes. In addition, the 1H-S(I_1) structures are 5.1 and 18.8 kJ mol^{-1} more stable than the second isomer, 1H-S(I_2) for water and ammonia clusters, respectively. The corresponding tautomer of the second isomer 2H-S is less stable by 13.4 (S=H_2O) and 13.1 kJmol^{-1} (S=NH_3) than the 1H-S(I_2) complexes in the ππ* state. As the relative stability is governed by the hydrogen-bonded network, we have also analyzed the

intermolecular interactions in the excited state. The ZPVE corrected binding energy $D_0(\pi\pi^*)$ of 1H-S(I_1) and 1H-S(I_2) isomers are 55.3 and 50.1 kJmol^{-1} (S=H_2O), and 62.3 and 43.5 kJmol^{-1} (S=NH_3), respectively. As seen in Table 1, the above values are much higher than those in S_0 states of the respective molecules. The above infers an increase in the hydrogen bond strength in the $\pi\pi^*$ state. To support the above, we have compared several structural parameters adjoining the hydrogen bonding sites that are mentioned in Table 1. In the excited state structures of 1H-S(I_1) isomers, the $R_{N(1)–Ha}$ bond length effectively lengthens by 0.016 (S=H_2O) and 0.022 Å (S=NH_3), and the $R_{N(7)\cdots Hb}$ distance shortens by 0.116 (S=H_2O) and 0.173 Å (S=NH_3) compared to the ground state structures. An increase of the $R_{N(1)–Ha}$ bond and a decrease of the $R_{N(7)\cdots Hb}$ certainly confirms a stronger hydrogen bonding. Similarly, the excited 7H-S isomers have shown a reduction in the $R_{N(7)\cdots Hb}$ length and an increase in the $R_{N(1)\cdots Ha}$ distance. The above observation supports the observed decrease in the dissociation energy $D_0(\pi\pi^*)$ values for the 7H-S isomer upon electronic excitation. In the case of 2H-S complexes, the $D_0(\pi\pi^*)$ values are marginally different from the ones in the ground state. This can be linked with the marginal change in the $R_{N(2)-H}$ bond lengths in the excited state.

M–S_2 complexes: The geometry optimized structures of the two-solvent clusters of 1H, 2H and 7H isomers in the lowest energy $\pi\pi^*$ state are shown in Figure 3. In this, the 1H-S_2(I_1) structures with N(1)–$H_a\cdots S_2\cdots$N(7) are ~20 kJmol^{-1} more stable than the 1H-S_2(I_2) structure with N(1)–$H_a\cdots S_2\cdots$N(2) linkages. The 1H-S_2(I_1) isomers are less stable by 62.1 and 72.9 kJmol^{-1} than their respective tautomeric 7H-W_2 and 7H-A_2 structures. The calculated binding energy data and the structural parameters are given in Table 1. The $D_0(\pi\pi^*)$ values the 1H-S_2(I_1) and 1H-S_2(I_2) complexes are found to be 119.0 and 95.8 kJmol^{-1} for water clusters and 95.9 and 77.5 kJmol^{-1} for ammonia clusters, respectively. The values are ~20-40 kJmol^{-1} higher than that in the ground state. The results fit well with the increased electron density of the N(7) and N(2) atoms in the $\pi\pi^*$ state, as described earlier. The 1H-S_2(I_1) structure shows an effective

increase of the $R_{N(1)–Ha}$ and decrease in $R_{N(7)\cdots Hb(S)}$ bond lengths (Table 1), suggesting a stronger hydrogen bonding interaction in the 1H-$S_2(I_1)$ complex. The $D_0(S_1)$ values of the corresponding tautomeric structures 7H-S_2 are 88.7 (S=H_2O) and 76.4 (S=NH_3) kJmol^{-1}. These values are ~15-20 kJmol^{-1} lower than the $D_0(S_0)$ of the complexes. However, the $D_0(\pi\pi^*)$ values for the 2H-S_2 complexes are marginally lesser than those in the ground state.

M–S_3 complexes: As shown in Table 1, the 7H-S_3 isomers are ~70 kJmol^{-1} more stable than the corresponding 1H-$S_3(I_1)$ isomers in the lowest energy $\pi\pi^*$ state. The $D_0(\pi\pi^*)$ values of the 1H-$S_3(I_1)$ complexes are 175.0 (S=H_2O) and 141.3 kJmol^{-1} (S=NH_3). The $D_0(\pi\pi^*)$ values of the corresponding tautomer complexes, 7H-S_3 are 149.2 (S=H_2O) and 118.3 kJmol^{-1}(S=NH_3), respectively. In addition, the $D_0(\pi\pi^*)$ values are higher by ~50-60 kJmol^{-1} in cases of 1H-$S_3(I_1)$ complexes and are lowered by 5-10 kJmol^{-1} in the 7H-S_3 complexes with respect to their corresponding ground state $D_0(S_0)$ values. The above implies a stronger hydrogen bonding interaction in the 1H-S_3 in the excited state. To support the above, the 1H-$S_3(I_1)$ cluster shows an effective increase of the $R_{N(1)–Ha}$ and decrease in $R_{N(7)\cdots Hb(S)}$ lengths upon electronic excitation. The $D_0(\pi\pi^*)$ values of the 1H-$S_3(I_2)$ complexes are 144.2 (S=H_2O) and 103.3 kJmol^{-1} (S=NH_3). The energies are ~30 kJmol^{-1} higher than those in the ground state. The respective tautomers 2H-S_3 are ~ 1.0 kJmol^{-1} less stable than 1H-$S_3(I_2)$ isomers in the $\pi\pi^*$ state.

3.3 The ground state hydrogen transfer energy barriers

In the ground state, the energy barriers (ZPVE corrected) associated with the 1H-to-7H and 1H-to-2H tautomerization reactions without any solvent molecule in the S_0 states were calculated to be 287.5 kJmol^{-1} and 368.0 kJmol^{-1}, respectively. In the case of R(1H-W_n-7H) pathways, the transition states are 91.2, 60.7, and 66.2 kJmol^{-1} (ZPVE corrected) for n=1, 2, and 3 complexes, respectively. In ammonia complexes, the transition barriers are 83.8, 73.8 and 69.6 kJmol^{-1} for n=1, 2 and 3, respectively. Similar energy barriers have been observed for R(1H-W_n-2H) reactions (SI Table S1). The inclusion of solvent-wire decreases the energy

barrier significantly. In the case of one solvent cluster, the energy barrier is higher than the calculated dissociation energies $D_0(S_0)$. The population of the 7H-S_n and 2H-S_n are negligible compared to the 1H-$S_n(I_1)$ isomer. All the above reactions are endothermic with high reaction barriers. Therefore, hydrogen transfer in the ground state is highly unlikely.

3.4 Excited-state hydrogen atom transfer reaction

3.4.1: 1H-S_n to 7H-S_n tautomerization reaction R(1H-S_n-7H)

The ESHT energy barriers without any solvent molecule in the ππ* states are high, i.e. 157.0 kJmol^{-1} for R(1H-7H) and 223.2 kJmol^{-1} for R(1H-2H)) and the channel is closed without either the involvement of solvent molecules or cyclic polymerization.[29] However, as reported before, the presence of a polar solvent enhances the tautomerization reaction in the excited state via hydrogen-bonded network. In the case of 1H-$S_{1\text{-}3}$ complexes, the excited state reaction pathway of the hydrogen transfer reaction is obtained via the constrained optimization along N(1)-H_a and N(7)-H_b bonds in the ππ* state states. This generates a 2D potential energy surface (2D-PES) in the ππ* state (SI Figure S4), and the lowest energy path connecting 1H-$S_n(I_1)$ and 7H-S_n complexes has been considered as the ESHT reaction R(1H-S_n-7H) channel as shown in Figure 5. The obtained energy data is likely to be more reliable than the computationally less expensive 1D-PES calculation using constrained optimization of the ππ* states for various intermediate structures reported earlier.[12]

Nevertheless, the transition state structures, i.e., the highest energy point on the reaction pathway in both 1D- and 2D surfaces, are found to be nearly identical. In three solvent systems, the 2D- reaction surface for R(1H-S_3-7H) is computationally demanding and often failed to converge in the excited state at the B3LYP level of theory. Systems where a 2D-PES could not be obtained such as in R(1H-S_3-7H), we have performed the 1D-PES calculations using constrained optimization of twelve intermediate structures between the reactant and product. The 1D-PES has been independently calculated in the R(1H-$S_{1\text{-}2}$-7H) systems, and the

transition states obtained are found to be nearly identical to the 2D-PES in energy and structures. Figure 5 shows the hydrogen transfer reaction R(1H-S_n-7H) as a function of N(7)-H_b bond distance. The highest energy structures in the 1D-PES are shown in Figure 6, and the structures are hereafter referred to as the transition states.

The calculated energy barriers in the R(1H-W_n-7H) reactions are 40, 27, and 26 kJmol^{-1} for n = 1, 2, and 3, respectively, as shown in Table 2. The excited-state energy barrier for one-water clusters in the excited ππ* state is similar to the one reported by Fang et al.[20] With an increase in the number of water molecules, the barrier height was found to be decreasing, and the relative energy of the resultant TS_{17}-W_2 has been obtained, similar to the reported value.[12] In the case of the R(1H-W_3-7H) reaction, the barrier height is expected to be lower than the TS_{17}-W_2 due to a better solvation factor. However, the energy barrier is nearly unchanged upon the addition of an extra water molecule. Similar observations have been attained for the $(NH_3)_{1-3}$ systems. In the case of R(1H-A_n-7H) reactions, the excited state hydrogen transfer reaction barriers are found to be 26, 15, and 14 kJmol^{-1}, respectively (Table 2). The successive addition of NH_3 molecules did not assure a gradual decrease in the barrier heights.

The addition of two or more solvent molecules significantly decreases the energy barrier of R(1H-S_n-7H) processes, suggesting a pronounced hydrogen transfer reaction via the formation of solvent wires. The energies of the transition state structures in the presence of multiple solvent molecules can be described using the following two characteristics: (a) the formation of a facile hydrogen-bonded network and (b) the relaxation of ∠C(8)-N(1)-H_a and ∠C(8)-N(7)-H_b angular tensions. The angles ∠C(8)-N(1)-H_a and ∠C(8)-N(7)-H_b are ~120±1° in the optimized structures of 1H-$S_n(I_1)$ and 7H-S_n in the S_1 state. A transition state structure with a similar ∠C(8)-N(1)-H_a and ∠C(8)-N(7)-H_b angles should have the lowest angle strain and low energy barrier. Any large-angle deviation can effectively increase the angle strain,

which therefore can increase the barrier heights. As shown in Table 2, the ∠C(8)-N(1)-H_a and ∠C(8)-N(7)-H_b angles in TS_{17}-W are both 104°, which are ~17° lower than the reference value. In the TS_{17}-W_2 structure (transition state in the $(H_2O)_2$ system), the bond angles remain nearly the same as in the 1H-$W_2(I_1)$ and 7H-W_2 structures. The higher energy of the TS_{17}-W (39.5 kJmol^{-1}) can be linked to the large angle strain in the structure. In the case of the TS_{17}-W_3 structure, bond angles are 10-12° higher than the reference value of 120°. As the barrier heights remained unchanged in R(1H-$S_{2/3}$-7H) systems, it can be implied that the solvation energy due to the extra water molecule can compensate for the angle strain in the transition state structures. Furthermore, the terminal N-H-O bond angles in the TS_{17}-$W_{2/3}$ transition states are nearly to 180° implying a favourable hydrogen bonding network. In the case of a single water cluster, the bond angles are ~160° and thus the hydrogen bond strength is expected to be less than the others. The stronger hydrogen bonding interaction in the TS_{17}-$W_{2/3}$ supports the observed stability of the transition states.

Similar to the 2,7DAI-$(H_2O)_n$-systems, the ESHT reactions R(1H-A_n-7H) in the ammonia system do not show a gradual decrease of the barrier energy on the successive addition of the solvent molecule. The structural parameters of the transition states are listed in Table 2. It is evident from the table that the ∠C(8)-N(1)-H_a and ∠C(8)-N(7)-H_b bond angles in TS_{17}-A are 11 and 17° lower than the reference value of 120°, implying a considerable angle strain in the structure. The bond angles are marginally higher in the TS_{17}-A_2 structure. In the case of the TS_{17}-A_3 structure, the bond angles are ~15° higher. As the barrier heights are similar in R(1H-$A_{2/3}$-7H) reactions, the angle strain in TS_{17}-A_3 is compensated by the gained solvation energy of the structure.

Substituting water with ammonia in the solvent wire effectively decreases the barrier heights (12-14 kJmol^{-1}). This is most likely due to the higher gas-phase basicity of the ammonia.[19] As shown in Table 2, both the N(1)-H_a and N(7)-H_b bonds in the transition states

are longer than the respective bonds in the 1H-S_n and 7H-S_n complexes. The above suggests an enhanced acidic character of the central DAI moiety in the transition state geometry. Therefore, the higher stability of TS_{17}-A_n is expected due to a stronger acid-base interaction compared to TS_{17}-W_n. Thus, the barrier heights are less in the ammonia complexes compared to the R(1H-W_n-7H) reactions.

The associated reaction paths are summarized in Figure 7. The barrier heights in R(1H-S_n-7H) reactions in the excited state are much lower than the corresponding dissociation energies $D_0(S_1)$ of the reactants 1H-$S_n(I_1)$, and the tautomerization process may proceed without any predissociation process. As shown in Figure 7, the 7H-S_n structures are > 60 kJmol^{-1} more stable than respective 1H-$S_n(I_1)$ structures. Therefore, the ESHT processes from 1H-$S_n(I_1)$ to 7H-S_n are thermodynamically favourable with energy barrier ranges from 14 to 40 kJmol^{-1}. The ESHT energy barriers are found to be lower with ammonia systems because of the higher gas-phase basicity of the molecule. Therefore, the rate of the ESHT process is expected to increase with the increased basicity of solvent molecules. Further, the energy barrier decreases significantly on addition of two or more solvent molecules. The addition of solvent molecules leads to a facile hydrogen transfer reaction, even though it doesn't ensure a gradual decrease in the barrier heights with an increasing number of solvent molecules.

3.4.2. 1H-S_n to 2H-S_n tautomerization reaction (R(1H-S_n-2H)):

The scope of the competing ESHT reaction R(1H-S_n-2H), where the hydrogen atom in N(1)-H group is transferred to the N(2) atom, depends on (i) the population of the 1H-$S_n(I_2)$ in the excited $\pi\pi^*$ state and (ii) the associated energy. As mentioned previously, the 1H-$S_n(I_2)$ is the second most stable isomer. Except for the 1H-$A_3(I_2)$, this second isomer is less stable by ~5-10 kJmol^{-1} in the ground state. The population of the second isomer is expected to be less, and therefore, the reaction R(1H-S_n-2H) that proceeds via the electronic excitation of 1H-$S_n(I_2)$

isomer appears to be a minor channel. In the ππ* state, 1H-$S_n(I_2)$ is more stable than the 2H-S_n product for each system, which makes the photochemical process thermodynamically less favourable. However, a conical intersection between the ππ* and nπ* states may lead to the more stable nπ* states of the tautomer 2H-S_n complexes. Therefore, there is a possibility of tautomerization process being thermodynamically favourable.

The solvation phase experiment found a strong fluorescence corresponding to the 2H tautomer formed in the aqueous medium.[15] Therefore, we have explored the R(1H-S_n-2H) transition barrier in the ππ* state. The 1H to 2H reaction without any solvent molecule is closed in the excited state because of the high energy barrier (223.2 kJmol^{-1}) of the reaction (Table 2). In the presence of the solvent molecules, the ESHT barrier heights were calculated between the 1H-$S_n(I_2)$ and 2H-S_n complexes using the 1D-PES (SI Figure S5) method described earlier. The energies associated with the R(1H-W-2H) reactions in the ππ* states are shown in Figure 7 and the structures of the transition state in Figure 8. In the case of R(1H-W-2H) reaction, the barrier height is found to be 127.4 kJmol^{-1} in the ππ* state, which is similar to the literature value of the ππ* state.[21] The successive addition of solvent molecules shows a decrease in the ESHT barrier heights to 83.1 and 35.6 kJmol^{-1} for R(1H-W_2-2H) and R(1H-W_3-2H) reactions, respectively. The energy barriers are significantly higher than the respective R(1H-W_n-7H) channels. In the case of the R(1H-$A_{1\text{-}3}$-2H) reaction, the energy barriers are 73.7, 42.8, and 31.2 kJmol^{-1}. The energies are 20-40 kJmol^{-1} higher than the competing R(1H-A_n-7H) reaction. In the reaction R(1H-S_n-2H), (a) the ground state population of the 1H-$S_n(I_2)$ is less compared to the 1H-$S_n(I_1)$ isomer and (b) the ESHT reaction barrier is high, and (c) the reaction marginally endothermic in nature. To investigate the conical intersection between the ππ* and nπ* states, the energies of the nπ* and ππ* states along the R(1H-S_n-2H) reaction pathways were plotted as a function of N_1-H_a bond distance (SI Figure S5). Here the energies of the nπ* states were calculated at the geometries optimized for the ππ* state. Except for the one-solvent

complexes, the conical intersection process occurs after the transition barriers along the reaction coordinate and, therefore, cannot alter the tautomerization reaction rate significantly. We can safely generalize that the 1H-$S_n(I_1)$ to 1H-$S_n(I_2)$ is a minor channel. Secondly, in the case of R(1H-S_n-2H), the reaction may proceed via an exothermic pathway to the nπ* state of 2H-S_n state. On the contrary, the nπ* state is an optically dark state (SI Table S3) and cannot be detected experimentally.

The experimental data of fluorescence emissions of 2H-S_n and 7H-S_n complexes reported [15] is the direct evidence for the possibility of excited-state hydrogen/proton transfer reactions because of the negligible ground state populations of both the tautomer complexes. The 7H tautomer is a product of ESHT from the 1H-$S_n(I_1)$ reactant. The population of the 1H-$S_n(I_2)$ isomer is expected to be lower than the most stable I_1 isomer. Considering the exothermicity and lower energy barrier in the excited state, it can be inferred that the R(1H-S_n-7H) is the primary hydrogen transfer reaction channel in the 2,7-DAI-S_n system. The reaction channel R(1H-S_n-2H) is a minor one because of the elevated energy barriers. The optically bright 2H-S_n complexes in the ππ* states are nearly endothermic. We must emphasize that the oscillator strength of the $S_0 \rightarrow S_{\pi\pi^*}$ transition in the 2H molecule is ~ 3 time higher than that in the 7H molecule. Hence, the strong fluorescence emission observed experimentally from 2H tautomer in the aqueous medium seems feasible. However, the reaction R(1H-S_n-2H) may lead to optically dark 2H-S_n complexes in the nπ* state.

5 Summary

In this article, we computationally explored the excited-state hydrogen atom transfer reactions in 2,7-diazaindole (DAI) – $(H_2O)_{1\text{-}3}$ and DAI – $(NH_3)_{1\text{-}3}$ isolated clusters. The study employed DFT and TDDFT calculation using B3LYP-D4/def2-TZVPP level of theory for the ground and excited state calculations, respectively. Without the solvent molecules, the

tautomerization reactions were found to be unachievable due to extremely large energy barriers. In 2,7-diazaindole, two competing ESHT reaction pathways R(1H-S_n-7H) and R(1H-S_n-2H) were investigated by increasing the length of the solvent wire connecting the hydrogen atom donor and acceptor groups. Both one- and two-dimensional potential energy surfaces were calculated in the excited state to investigate the pathways. The R(1H-S_n-7H) was found to be the dominant pathway with the reaction barriers ranging from 14-27 kJmol^{-1} and 26.0-39.5 kJmol^{-1} with ammonia and water molecules as solvents, respectively. The lengthening of the solvent chain up to two molecules depicted a drastic decrease of ~12 kJmol^{-1} in the barrier heights. The R(1H-A_2-7H) reaction barrier was found at 15 kJmol^{-1}, which was nearly half of the barrier heights calculated in the respective water cluster. The barrier of the minor reaction channel R(1H-S_n-2H) was significantly higher (31-127 kJmol^{-1}) than the other and was found to be decreasing with the increasing length of the solvent wire.

It is evident from the discussion that the primary channel for the excited-state hydrogen transfer in the 2,7-DAI-S_n system is R(1H-S_n-7H). The possibility of the competing reaction R(1H-S_n-2H) is very low because of (a) lower population of 1H-S_n(I_2) in the ground state and (b) the high energy barrier in the excited state. In both the reactions, the angle strains present in the transition state structures were found to be directly linked to the length of the solvent chain and most likely govern the barrier heights in the reactions. The efficient ESHT process in R(1H-S_n-7H) and R(1H-S_n-2H) reactions require at least two and three solvent molecules, respectively. Any further addition of solvent molecules may result in an increased angle strain and thus may not facilitate the ESHT reactions. We have also concluded that the ammonia molecule is a better candidate for hydrogen transfer compared to water because of its higher gas-phase basicity. The calculated data can be used as a reference for the gas phase experimental community to investigate the energetics and dynamics of solvent-mediated hydrogen atom transfer reactions in the photoexcited states. The findings of this study are

expected to be crucial to understand the ESHT reaction pathways in N-H containing biorelevant molecules.

Supporting Information Available: The ground state structures and energies are discussed in the supporting information document. The coordinates of all the excited state geometries are listed.

CRediT author statement:

Simran Baweja: Methodology, Validation, Data curation, Writing - Original Draft
Prahlad Roy Chowdhury: Methodology, Formal analysis, Writing - Original Draft.
Surajit Maity: Conceptualization, Supervision, Writing - Review & Editing

Acknowledgment:

SB thanks MHRD, Government of India for the fellowship. PRC and SM thanks IIT Hyderabad and SERB, DST for fellowship

Funding: This work was supported by SERB, DST, Government of India (Grant no. CRG/2019/003335)

References:

[1] F. Yu, P. Li, G. Li, G. Zhao, T. Chu, K. Han, A near-IR reversible fluorescent probe modulated by selenium for monitoring peroxynitrite and imaging in living cells, J. Am. Chem. Soc. 133 (2011) 11030–11033. https://doi.org/10.1021/ja202582x.

[2] F. Yu, P. Li, B. Wang, K. Han, Reversible near-infrared fluorescent probe introducing tellurium to mimetic glutathione peroxidase for monitoring the redox cycles between peroxynitrite and glutathione in vivo, J. Am. Chem. Soc. 135 (2013) 7674–7680. https://doi.org/10.1021/ja401360a.

[3] J. Wu, W. Liu, J. Ge, H. Zhang, P. Wang, New sensing mechanisms for design of fluorescent chemosensors emerging in recent years, Chem. Soc. Rev. 40 (2011) 3483–3495. https://doi.org/10.1039/c0cs00224k.

[4] D. Tuna, N. Došlić, M. Mališ, A.L. Sobolewski, W. Domcke, Mechanisms of photostability in kynurenines: A joint electronic-structure and dynamics study, J. Phys. Chem. B. 119 (2015) 2112–2124. https://doi.org/10.1021/jp501782v.

[5] P. Chou, Y. Chi, Phosphorescent Dyes for Organic Light-Emitting Diodes, Chem. Eur. J. 13 (2007) 380–395. https://doi.org/10.1002/chem.200601272.

[6] J. Li, Y. Wu, Z. Xu, Q. Liao, H. Zhang, Y. Zhang, L. Xiao, J. Yao, H. Fu, Tuning the organic microcrystal laser wavelength of ESIPT-active compounds: Via controlling the excited enol∗ and keto∗ emissions, J. Mater. Chem. C. 5 (2017) 12235–12240. https://doi.org/10.1039/c7tc04207h.

[7] Z. Gao, W. Zhang, Y. Yan, J. Yi, H. Dong, K. Wang, J. Yao, Y.S. Zhao, Proton-Controlled Organic Microlaser Switch, ACS Nano. 12 (2018) 5734–5740. https://doi.org/10.1021/acsnano.8b01607.

[8] Y. Yang, J. Zhao, Y. Li, Theoretical Study of the ESIPT Process for a New Natural Product Quercetin, Sci. Rep. 6 (2016) 1–9. https://doi.org/10.1038/srep32152.

[9] J.E. Kwon, S.Y. Park, Advanced organic optoelectronic materials: Harnessing excited-state intramolecular proton transfer (ESIPT) process, Adv. Mater. 23 (2011) 3615–3642. https://doi.org/10.1002/adma.201102046.

[10] D.R. Weinberg, C.J. Gagliardi, J.F. Hull, C.F. Murphy, C.A. Kent, B.C. Westlake, A. Paul, D.H. Ess, D. Granville, T.J. Meyer, Proton-Coupled Electron Transfer, Chem. Rev 112 (2012) 4016-4093 . htttps://doi.org/10.1021/cr200177j.

[11] E. Freier, S. Wolf, K. Gerwert, Proton transfer via a transient linear water-molecule chain in a membrane protein, Proc. Natl. Acad. Sci. U. S. A. 108 (2011) 11435–11439. https://doi.org/10.1073/pnas.1104735108.

[12] Y. Liu, Z. Tang, Y. Wang, J. Tian, X. Fei, F. Cao, G.Y. Li, Theoretical study of excited-state proton transfer of 2,7-diazaindole·(H2O)2 cluster via hydrogen bonding dynamics, Spectrochim. Acta - Part A Mol. Biomol. Spectrosc. 187 (2017) 163–167. https://doi.org/10.1016/j.saa.2017.06.052.

[13] J. Yi, H. Fang, Effect of different alkyl groups on excited-state tautomerization of 7AI-azaindole-H2O: A theoretical study, Spectrochim. Acta - Part A Mol. Biomol. Spectrosc. 202 (2018) 58–64. https://doi.org/10.1016/j.saa.2018.05.037.

[14] Z. Tang, Y. Qi, Y. Wang, P. Zhou, J. Tian, X. Fei, Excited-State Proton Transfer Mechanism of 2,6-Diazaindoles·(H2O)n (n = 2-4) Clusters, J. Phys. Chem. B. 122 (2018) 3988–3995. https://doi.org/10.1021/acs.jpcb.7b10207.

[15] J.Y. Shen, W.C. Chao, C. Liu, H.A. Pan, H.C. Yang, C.L. Chen, Y.K. Lan, L.J. Lin, J.S. Wang, J.F. Lu, S. Chun-Wei Chou, K.C. Tang, P.T. Chou, Probing water micro-solvation in proteins by water catalyzed proton-transfer tautomerism. Nat Commun. 4 (2013) 1-7. https://doi.org/10.1038/ncomms3611.

[16] P. Meredith, T. Sarna, The physical and chemical properties of eumelanin, Pigment Cell Res. 19 (2006) 572–594. https://doi.org/10.1111/j.1600-0749.2006.00345.x.

[17] O. Plekan, H. Sa'adeh, A. Ciavardini, C. Callegari, G. Cautero, C. Dri, M. Di Fraia, K.C. Prince, R. Richter, R. Sergo, L. Stebel, M. Devetta, D. Faccialà, C. Vozzi, L. Avaldi, P. Bolognesi, M.C. Castrovilli, D. Catone, M. Coreno, F. Zuccaro, E. Bernes, G. Fronzoni, D. Toffoli, A. Ponzi, Experimental and Theoretical Photoemission Study of Indole and Its Derivatives in the Gas Phase, J. Phys. Chem. A. 124 (2020) 4115–4127. https://doi.org/10.1021/acs.jpca.0c02719.

[18] S. Yamazaki, Concerted-asynchronous reaction path of the excited-state transfer in the 7-azaindole homodimer and 6H-indolo[2,3-b]quinoline/7-azaindole heterodimer, Chem. Phys. 515 (2018) 768–778. https://doi.org/10.1016/j.chemphys.2017.11.009.

[19] P.J. Linstrom and W.G. Mallard, Eds., NIST Chemistry WebBook, NIST Standard Reference Database Number 69, National Institute of Standards and Technology, Gaithersburg MD, 20899, https://doi.org/10.18434/T4D303

[20] H. Fang, Y. Kim, Excited-state tautomerization in the 7-azaindole-(H2O) n (n = 1 and 2) complexes in the gas phase and in solution: A theoretical study, J. Chem. Theory Comput. 7 (2011) 642–657. https://doi.org/10.1021/ct100647b.

[21] H. Fang, Halogen substituent effect on the water-assisted excited-state tautomerization of 2, 7-diazaindole-H 2 O complex in aqueous solution: A theoretical study, Spectrochim. Acta - Part A Mol. Biomol. Spectrosc. 214 (2019) 152–160. https://doi.org/10.1016/j.saa.2019.02.016.

[22] H. Fang, A theoretical study on water-assisted excited state double proton transfer process in substituted 2,7-diazaindole-H2O complex, Theor. Chem. Acc. 139 (2020) 139.

https://doi.org/10.1007/s00214-020-02655-3.

[23] AD Becke, Density-functional thermochemistry. III. The role of exact exchange, J. Chem. Phys. 98 (1993) 5648–5652. https://doi.org/10.1063/1.464913.

[24] B. Miehlich, A. Savin, H. Stoll, H. Preuss, Results obtained with the correlation energy density functionals of becke and Lee, Yang and Parr , Chem. Phys. Lett. 157 (1989) 200–206. https://doi.org/10.1016/0009-2614(89)87234-3.

[25] Lee, Chengteh and Yang, Weitao and Parr, Robert G, Development of the Colle-Salvetti correlation-energy formula into a functional of the electron density, Phys. Rev. B 37 (1988) 785–789. https://doi.org/10.1103/PhysRevB.37.785.

[26] A. Schäfer, H. Horn, R. Ahlrichs, Fully optimized contracted Gaussian basis sets for atoms Li to Kr, J. Chem. Phys. 97 (1992) 2571–2577. https://doi.org/10.1063/1.463096.

[27] A. Schäfer, C. Huber, R. Ahlrichs, Fully optimized contracted Gaussian basis sets of triple zeta valence quality for atoms Li to Kr, J. Chem. Phys. 100 (1994) 5829–5835. https://doi.org/10.1063/1.467146.

[28] R. Ahlrichs, M. Bär, M. Häser, H. Horn, C. Kölmel, Electronic structure calculations on workstation computers: The program system turbomole, Chem. Phys. Lett. 162 (1989) 165–169. https://doi.org/10.1016/0009-2614(89)85118-8.

[29] S. Takeuchi, T. Tahara, Femtosecond ultraviolet-visible fluorescence study of the excited-state proton-transfer reaction of 7-azaindole dimer, J. Phys. Chem. A. 102 (1998) 7740–7753. https://doi.org/10.1021/jp982522v.

Simran Baweja: Methodology, Validation, Data curation, Writing - Original Draft

Prahlad Roy Chowdhury: Methodology, Formal analysis, Writing - Original Draft.

Surajit Maity: Conceptualization, Supervision, Writing - Review & Editing

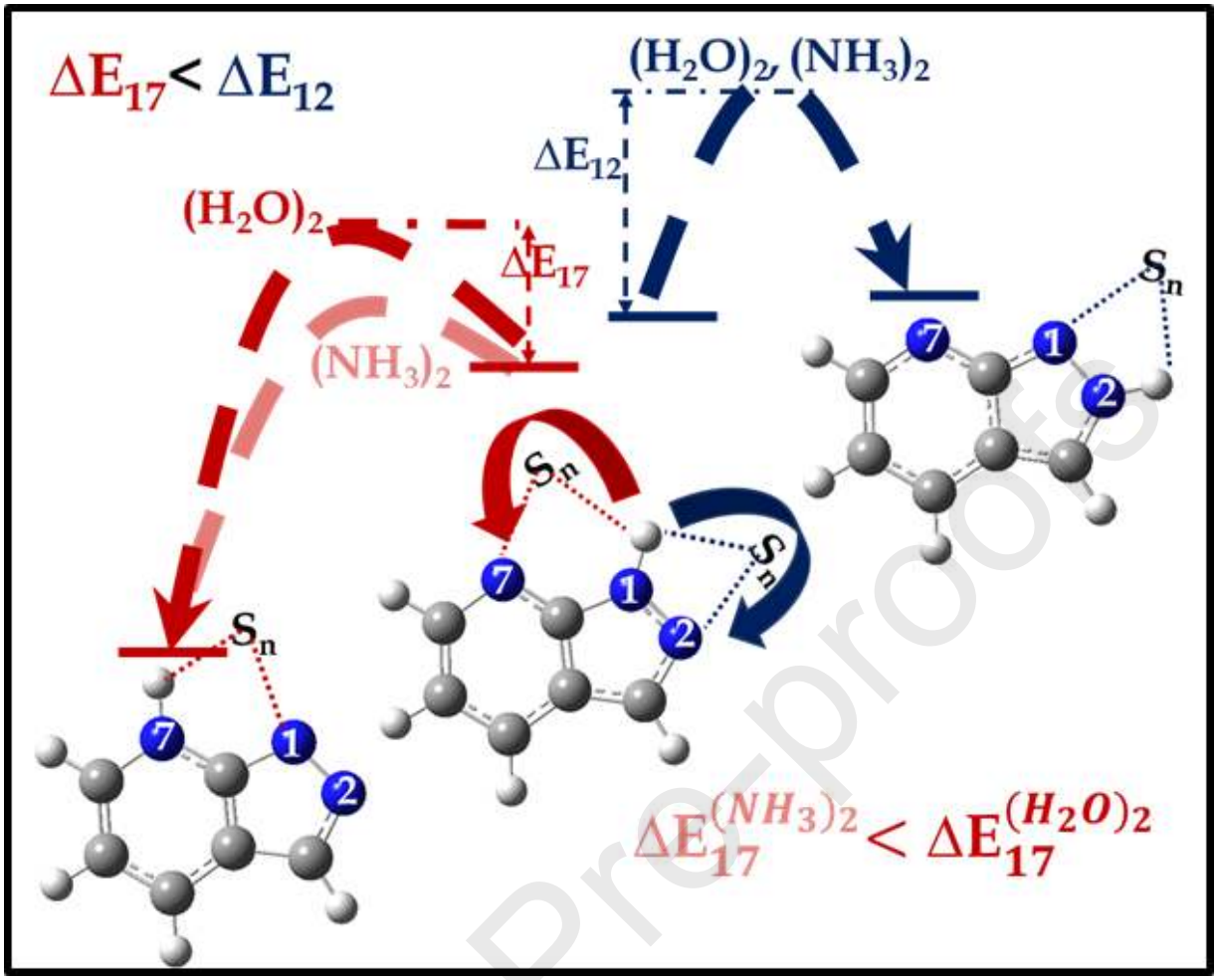

TABLE 1: The relative (ΔE_r (S_0) and ΔE_r (S_1)), binding ($D_0(\pi\pi^*)$ and $D_0(S_0)$) energies (in kJmol^{-1}) of the optimized structures of 1H, 7H and 2H isomers of 2,7-DAI and the S_{1-3} clusters (S=W for water, S=A for ammonia) in the ground S_0 and electronically excited $\pi\pi^*$ state. All the energies are ZPVE corrected. The N_1-H, N_7-H and N_2-H covalent and the closest hydrogen bond distances in the $\pi\pi^*$ states are given. The numbers in italics correspond to that in the ground state structures. The energy values in parentheses for 2H-S_n clusters signify the relative energy with respect to the corresponding 1H-$S_n(I_2)$ isomer.

Name	**1H**	**7H**	**2H**					
ΔE_r ($\pi\pi^*$)	0.0	-92.4	0.6					
ΔE_r (S_0)	*0.0*	*76.5*	*32.6*					
$R_{N(1)–Ha}$ / $R_{N(2/7)–Hb}$	1.012 (*1.004*)	1.004 (*1.010*)	1.001 (*1.006*)					
Name	**1H-W(I_1)**	**7H-W**	**1H-W(I_2)**	**2H-W**	**1H-A(I_1)**	**7H-A**	**1H-A(I_2)**	**2H-A**
ΔE_r ($\pi\pi^*$)	**0.0**	**-75.6**	**5.1**	**18.5 (13.4)**	**0.0**	**-74.4**	**18.8**	**31.9 (13.1)**
ΔE_r (S_0)	*0*	*56.9*	*10.2*	*34.8 (24.6)*	*0*	*57.9*	*5.2*	*29.7 (24.5)*
$D_0(\pi\pi^*)$ (kJmol^{-1})	**-55.3**	**-38.5**	**-50.1**	**-37.4**	**-62.3**	**-44.2**	**-43.5**	**-31.1**
***$D_0(S_0)$* (kJmol^{-1})**	*-35.9*	*-55.8*	*-25.8*	*-33.6*	*-33.8*	*-52.7*	*-28.7*	*-36.6*
$R_{N(1)–Ha}$ / $R_{N(1)\cdots Ha}$	1.028 (*1.012*)	1.985 (*1.870*)	1.020 (*1.010*)	2.124 (*2.060*)	1.043 (*1.021*)	2.410 (*2.222*)	1.042 (*1.022*)	2.835 (*2.664*)
$R_{N(7)–Hb}$ / $R_{N(7)\cdots Hb}$	1.854 (*1.970*)	1.014 (*1.026*)	-	-	2.257 (*2.430*)	1.023 (*1.038*)	-	-
$R_{N(2)–Hb}$ / $R_{N(2)\cdots Hb}$	-	-	2.172 (*2.085*)	1.010 (*1.013*)	-	-	3.202 (*3.119*)	1.023 (*1.025*)
Name	**1H-$W_2(I_1)$**	**7H-W_2**	**1H-$W_2(I_2)$**	**2H-W_2**	**1H-$A_2(I_1)$**	**7H-A_2**	**1H-$A_2(I_2)$**	**2H-A_2**
ΔE_r ($\pi\pi^*$)	**0.0**	**-62.1**	**23.2**	**24.0 (0.8)**	**0.0**	**-72.9**	**18.4**	**28 (9.6)**
ΔE_r (S_0)	*0.0*	*45.5*	*9.3*	*26.7 (17.4)*	*0.0*	*51.3*	*5.0*	*22.9 (17.9)*
$D_0(\pi\pi^*)$ (kJmol^{-1})	**-119.0**	**-88.7**	**-95.8**	**-95.6**	**-95.9**	**-76.4**	**-77.5**	**-68.4**
***$D_0(S_0)$* (kJmol^{-1})**	*-80.1*	*-111.4*	*-70.8*	*-86.1*	*-64.8*	*-90.3*	*-59.8*	*-74.3*
$R_{N(1)–Ha}$ / $R_{N(1)\cdots Ha}$	1.051 (*1.026*)	1.800 (*1.740*)	1.040 (*1.024*)	1.892 (*1.850*)	1.070 (*1.038*)	2.151 (*2.034*)	1.069 (*1.037*)	2.211 (*2.140*)
$R_{N(7)–Hb}$ / $R_{N(7)\cdots Hb}$	1.713 (*1.818*)	1.025 (*1.041*)	-	-	2.033 (*2.132*)	1.034 (*1.054*)	-	-
$R_{N(2)–Hb}$ / $R_{N(2)\cdots Hb}$	-	-	1.943 (*1.876*)	1.026 (*1.028*)	-	-	2.273 (*2.188*)	1.041 (*1.040*)
Name	**1H-$W_3(I_1)$**	**7H-W_3**	**1H-$W_3(I_2)$**	**2H-W_3**	**1H-$A_3(I_1)$**	**7H-A_3**	**1H-$A_3(I_2)$**	**2H-A_3**
ΔE_r ($\pi\pi^*$)	**0.0**	**-66.6**	**30.8**	**31.8 (1.0)**	**0.0**	**-69.5**	**38.0**	**39.0 (1.0)**

ΔE$_r$ (S$_0$)	*0.0*	*42.2*	*4.0*	*18.7 (14.7)*	*0.0*	*49.6*	*-0.4*	*18.1 (18.5)*
D$_0$(ππ*) (kJmol^{-1})	**-175.0**	**-149.2**	**-144.2**	**-143.8**	**-141.3**	**-118.3**	**-103.3**	**-102.8**
***D$_0$(S$_0$)* (kJmol^{-1})**	*-113.1*	*-147.8*	*-109.1*	*-126.9*	*-82.6*	*-109.9*	*-83.1*	*-97.1*
$R_{N(1)–Ha}$ / $R_{N(1)\cdots Ha}$	1.056 (*1.029*)	1.819 (*1.731*)	1.052 (*1.031*)	1.823 (*1.802*)	1.079 (*1.041*)	2.139 (*2.044*)	1.084 (*1.043*)	2.193 (*2.101*)
$R_{N(7)–Hb}$ / $R_{N(7)\cdots Hb}$	1.692 (*1.792*)	1.028 (*1.041*)	-	-	2.029 (*2.122*)	1.038 (*1.058*)	-	-
$R_{N(2)–Hb}$ / $R_{N(2)\cdots Hb}$	-	-	1.864 (1.813)	1.034 (*1.034*)	-	-	2.189 (*2.135*)	1.055 (*1.045*)

Table 2: Energies and structural parameters of the possible transition states found in excited state tautomerization pathways from 1H-S_n to 7H-Sn, and 2H-S_n complexes.

Name	**TS_{17}**		**Name**	**TS_{12}**	
ΔE_r (kJmol^{-1})	157.0		**ΔE_r (kJmol^{-1})**	223.2	
$\angle$C(8)-N(1)-H_a	71.6		**$\angle$N(2)-N(1)-H_a**	68.0	
$\angle$C(8)-N(7)-H_b	72.9		**$\angle$N(1)-N(2)-H_b**	57.5	
Name	**TS_{17}-W**	**TS_{17}-A**	**Name**	**TS_{12}-W**	**TS_{12}-A**
ΔE_r (kJmol^{-1})	39.5	26.0	**ΔE_r (kJmol^{-1})**	127.4	73.7
$\angle$C(8)-N(1)-H_a	103.8	109.2	**$\angle$N(2)-N(1)-H_a**	89.9	99.8
$\angle$C(8)-N(7)-H_b	104.0	103.0	**$\angle$N(1)-N(2)-H_b**	95.8	86.5
$R_{N(1)-Ha}$	1.328	1.224	**$R_{N(1)-Ha}$**	1.553	1.660
$R_{N(7)-Hb}$	1.288	1.423	**$R_{N(2)-Hb}$**	1.397	2.364
Name	**TS_{17}-W_2**	**TS_{17}-A_2**	**Name**	**TS_{12}-W_2**	**TS_{12}-A_2**
ΔE_r (kJmol^{-1})	27.0	15.0	**ΔE_r (kJmol^{-1})**	83.1	42.8
$\angle$C(8)-N(1)-H_a	124.2	126.0	**$\angle$N(2)-N(1)-H_a**	111.0	117.6
$\angle$C(8)-N(7)-H_b	121.1	122.1	**$\angle$N(1)-N(2)-H_b**	114.7	107.0
$R_{N(1)-Ha}$	1.270	1.370	**$R_{N(1)-Ha}$**	1.338	1.680
$R_{N(7)-Hb}$	1.525	1.900	**$R_{N(2)-Hb}$**	1.246	1.597
Name	**TS_{17}-W_3**	**TS_{17}-A_3**	**Name**	**TS_{12}-W_3**	**TS_{12}-A_3**
ΔE_r (kJmol^{-1})	26.0	14.0	**ΔE_r (kJmol^{-1})**	35.6	31.2
$\angle$C(8)-N(1)-H_a	133.1	135.1	**$\angle$N(2)-N(1)-H_a**	120.5	134.3
$\angle$C(8)-N(7)-H_b	131.1	134.2	**$\angle$N(1)-N(2)-H_b**	118.1	114.0
$R_{N(1)-Ha}$	1.653	1.560	**$R_{N(1)-Ha}$**	1.432	1.786
$R_{N(7)-Hb}$	1.703	1.911	**$R_{N(2)-Hb}$**	1.294	1.467

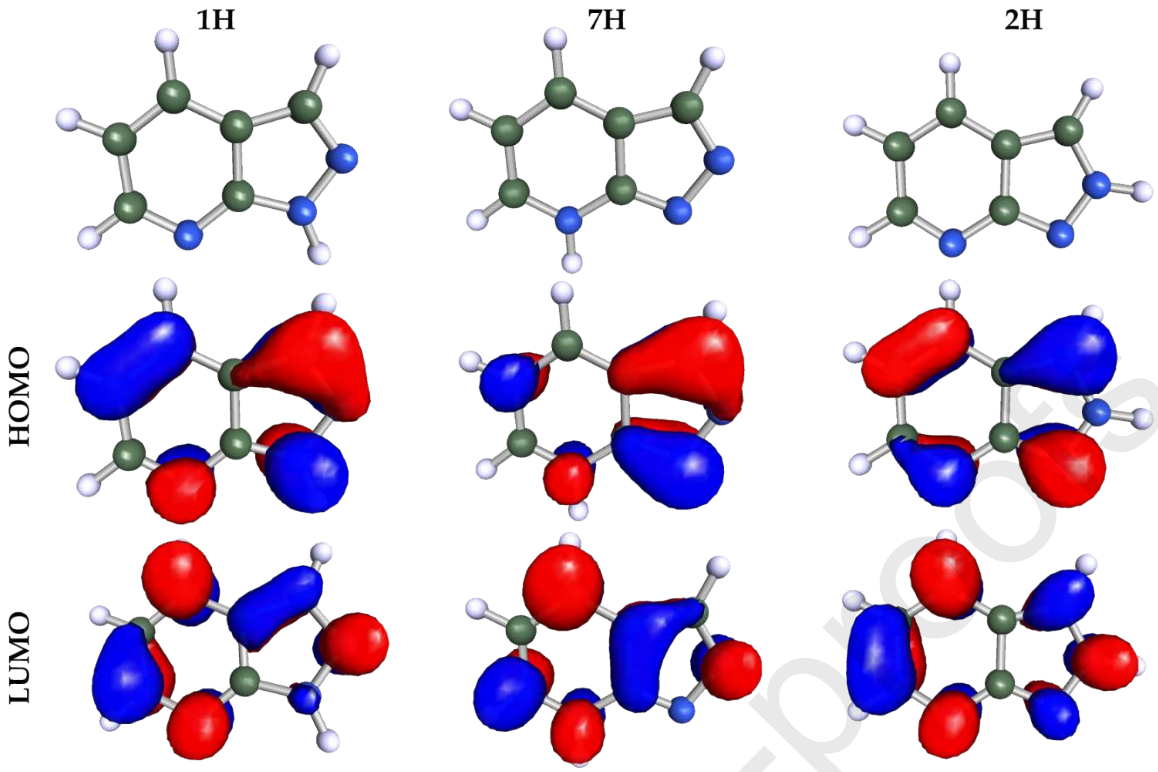

Figure 1: The optimized structures of 2,7-DAI (1H) and its tautomers 7H and 2H with the HOMO and LUMO molecular orbitals. The blue, green, and white balls represent nitrogen, carbon and hydrogen atoms, respectively.

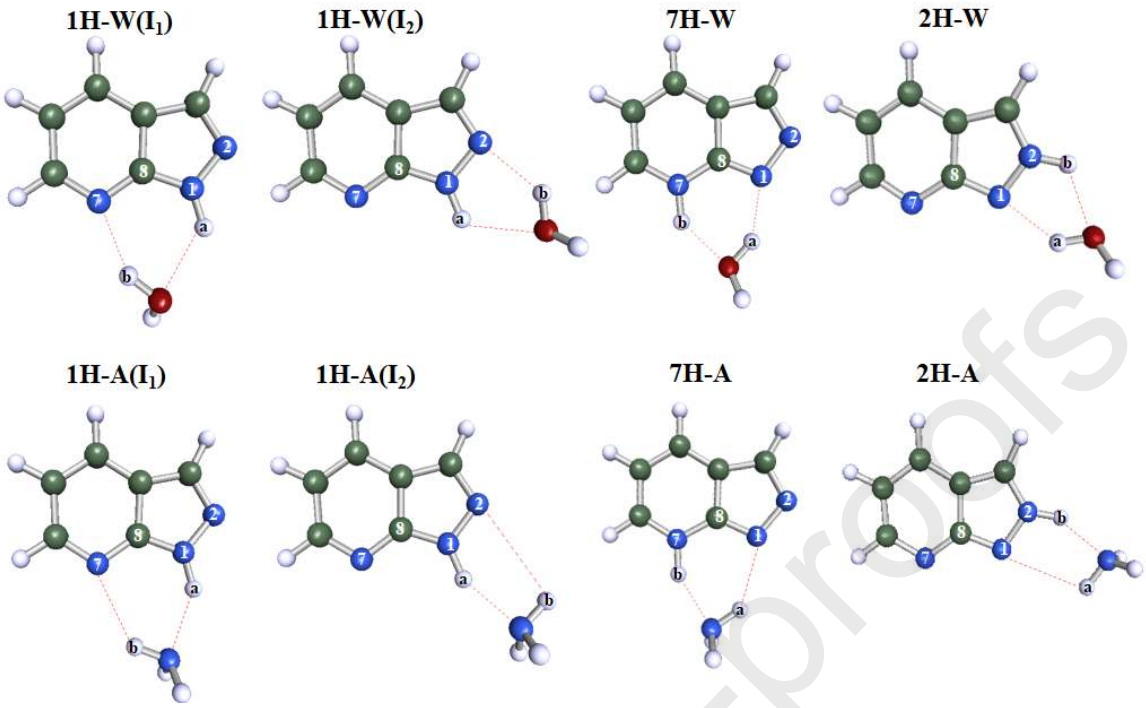

Figure 2: Excited state geometries of the most stable 1H–S (I_1 and I_2), 7H-S and 2H-S (S= W for H_2O and S = A for NH_3) structures. The bonded H atoms to (i) the N(1) atom is labelled as 'a' and (ii) the N(2) or N(7) is labelled as 'b'. The red, blue, green, and white balls represent oxygen, nitrogen, carbon and hydrogen atoms.

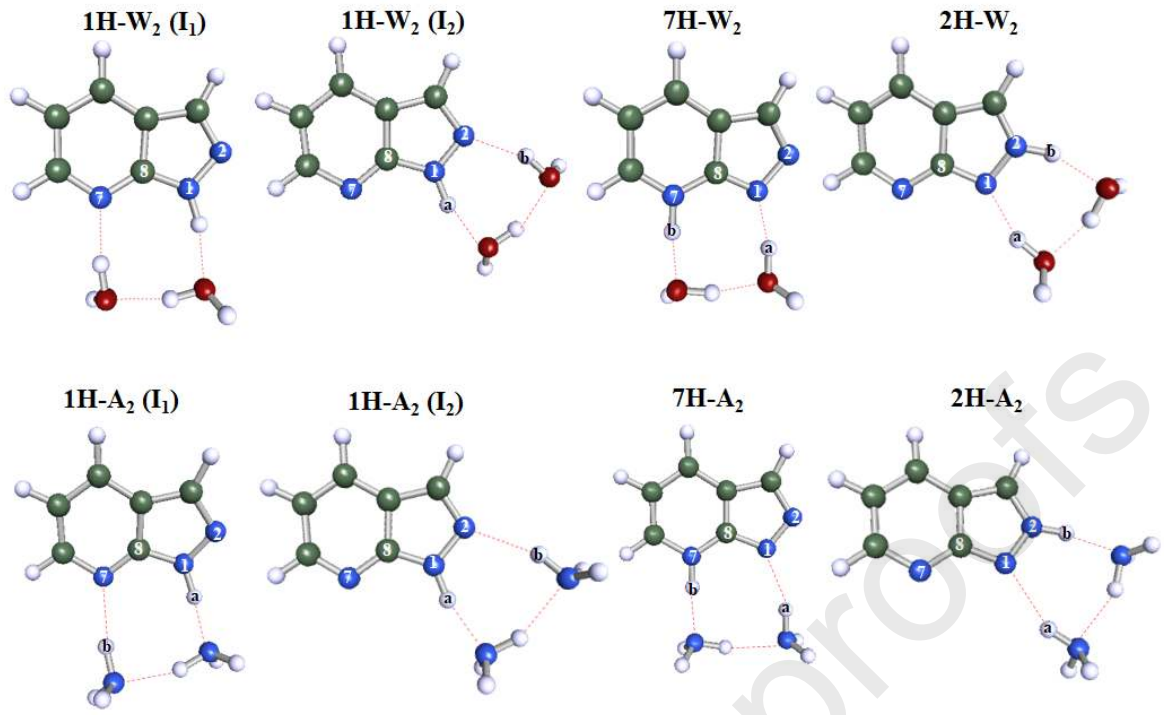

Figure 3: Excited state geometries of the most stable 1H–S_2 (I_1 and I_2), 7H-S_2 and 2H-S_2 (S= W for H_2O and S = A for NH_3) structures. The bonded H atoms to (i) the N(1) atom is labelled as 'a' and (ii) the N(2) or N(7) is labelled as 'b'. The red, blue, green, and white balls represent oxygen, nitrogen, carbon and hydrogen atoms, respectively.

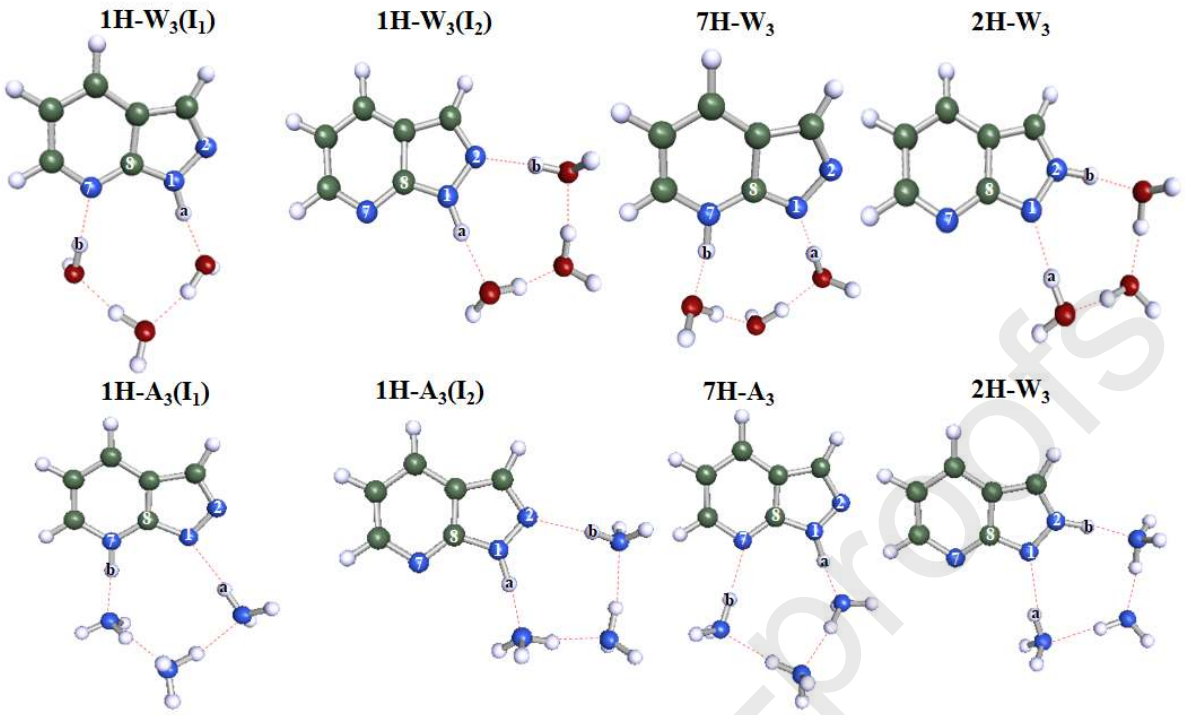

Figure 4: Excited state geometries of the most stable 1H–S_3 (I_1 and I_2), 7H-S_3 and 2H-S_3 (S= W for H_2O and S = A for NH_3) structures. The bonded H atoms to (i) the N(1) atom is labelled as 'a' and (ii) the N(2) or N(7) is labelled as 'b'. The red, blue, green, and white balls represent oxygen, nitrogen, carbon and hydrogen atoms, respectively.

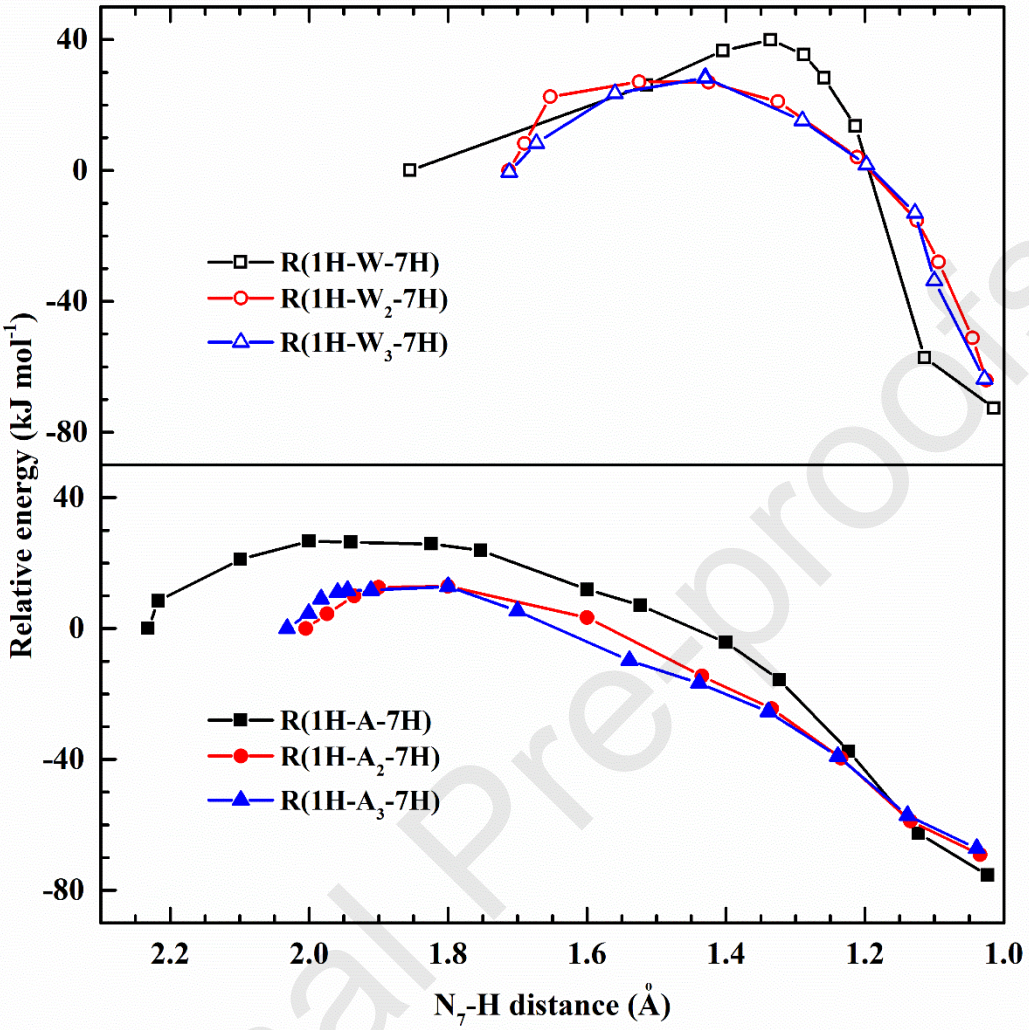

Figure 5: The energies of the ππ* states along the excited state hydrogen transfer pathways between the 1H-S_n to 7H-S_n isomers.

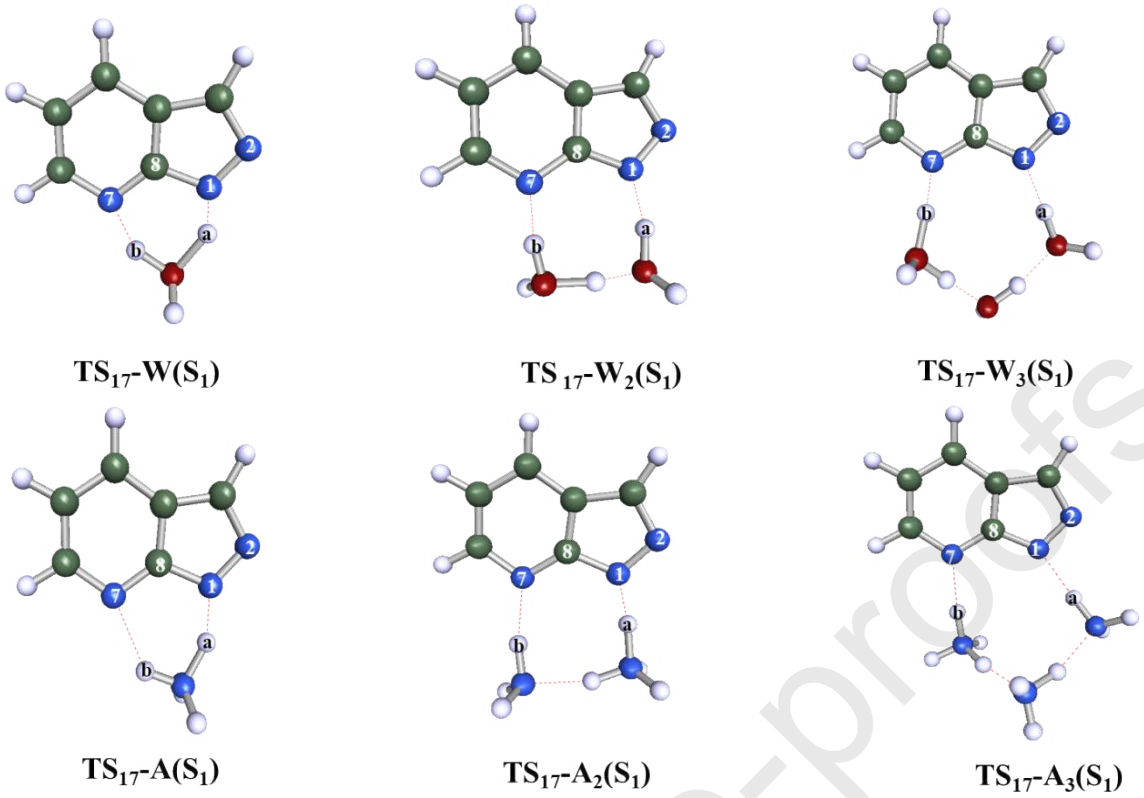

Figure 6: The transition states in the ESHT in 27DAI-S_n (n=1-3) clusters (W for H_2O, A for NH_3).

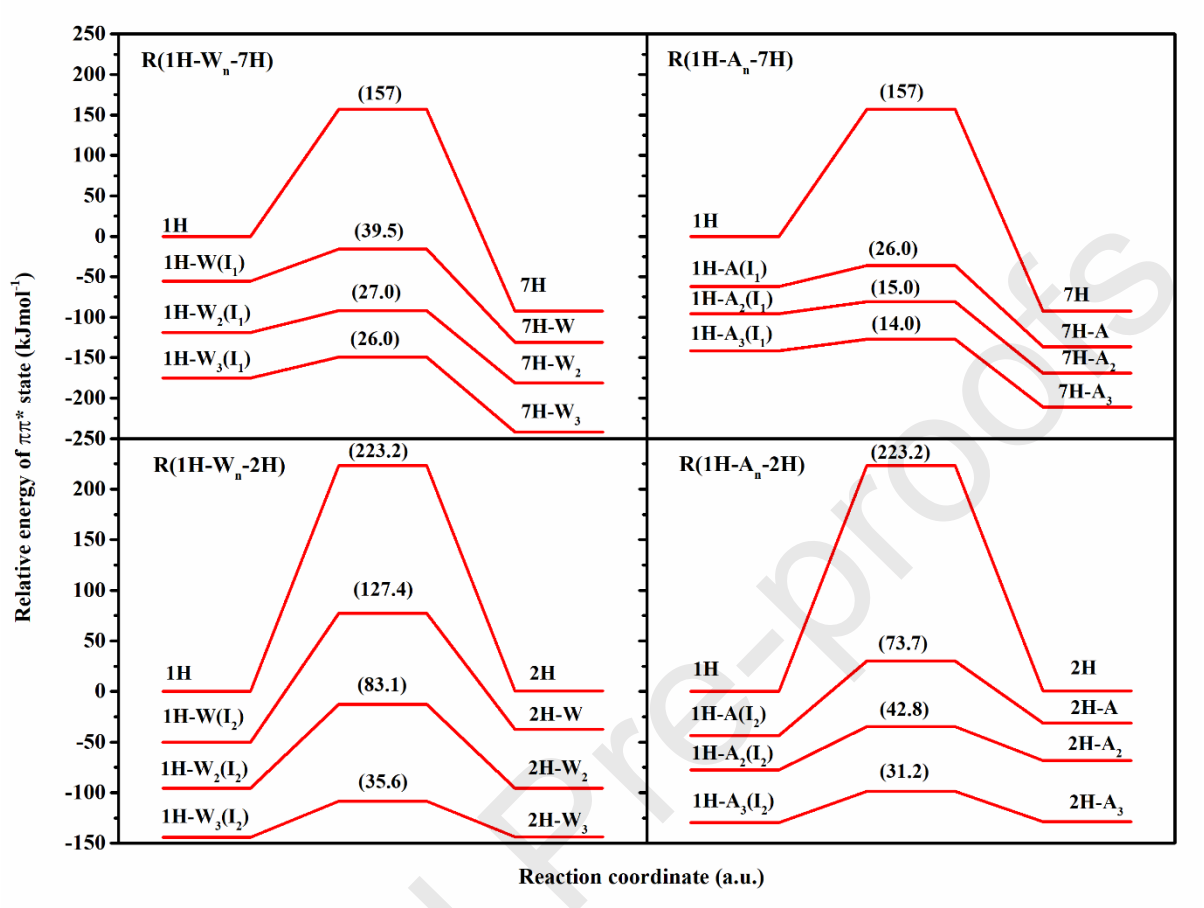

Figure 7: The relative energies of the ESHT reactions in the ππ* state. In each reaction, the energies of the reactants and products are relative to the ππ* energy state of the bare 1H isomer. The transition state energy is relative to the ππ* state of the reactant on the left side for each system.

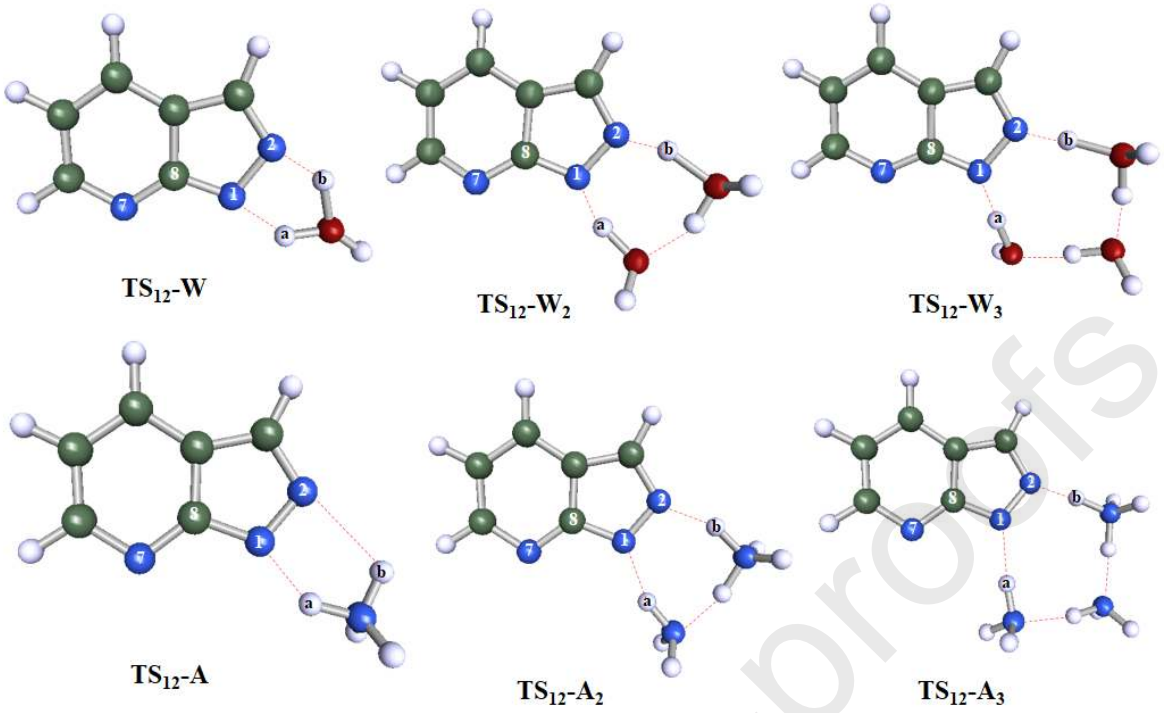

Figure 8: The transition states in the ESHT process R(1H-S_n-2H) in 27DAI-S_n (n=1-3) clusters (W for H_2O, A for NH_3).

Declaration of interests

☒ The authors declare that they have no known competing financial interests or personal relationships that could have appeared to influence the work reported in this paper.

☐The authors declare the following financial interests/personal relationships which may be considered as potential competing interests: